

A ^1H and ^{13}C Solid State NMR Investigation of the Structure and Molecular Dynamics of Hydrogenated Oligocyclopentadiene

Claudia Forte,^{*,†} Marco Geppi,[‡] Alessandro Triolo,[§] Carlo Alberto Veracini,[‡] and Giuseppe Visalli[‡]

Istituto di Chimica Quantistica ed Energetica Molecolare, CNR, via Risorgimento 35, 56126 Pisa, Italy; Dipartimento di Chimica e Chimica Industriale, Università degli Studi di Pisa, via Risorgimento 35, 56126 Pisa, Italy; and Department of Chemistry, Heriot Watt University, Riccarton, Edinburgh EH14 4AS, United Kingdom

Received: August 24, 1999

The structure and dynamics of hydrogenated oligo(cyclopentadiene) (HOCP) was investigated by means of ^1H and ^{13}C NMR in the solid state. The ^{13}C NMR spectrum of HOCP is reported and interpreted for the first time here. Quantitative information on the distribution of the different structural and diastereoisomeric environments of the cyclopentane monomers was thus obtained. Moreover, the dynamic behavior of HOCP was investigated through the measurements of ^1H $T_{1\rho}$ and T_1 , as well as ^{13}C T_1 relaxation times, highlighting the presence of two major motional processes, whose specific nature is discussed. Quantitative dynamic parameters were extracted by applying suitable theoretical models to the ^1H T_1 curve vs temperature.

Introduction

Recently, HOCP has been thoroughly studied, but essentially as a blend constituent: a large amount of work has been devoted to the understanding of the morphology and phase diagrams of its blends with isotactic polypropylene (iPP),¹ high-density polyethylene (HDPE),² and poly(4-methylpentene) (P4MP1). The mixtures between HOCP and these polymers have shown a peculiar behavior, as for example the occurrence of a phase immiscibility loop in some of the blends (iPP–HOCP and HDPE–HOCP): it has been shown that these mixtures present both an upper and lower consolution point as a function of both composition and temperature. From a morphological point of view, small-angle X-ray and Neutron scattering techniques allowed to characterize the coexistence of two different lamellar domains when the mixture lies inside the miscibility gap.

In order to further investigate the nature of the interaction between high molecular weight polymers and HOCP, it is important to understand the structural and dynamic properties of the low molecular weight additive, but, in spite of the numerous studies performed on blends, chemophysical characterizations of pure HOCP are scarce or completely absent, and NMR experiments in particular are lacking.

In this paper, HOCP was investigated by means of ^1H and ^{13}C solid state NMR, a technique which is known to give important information both from a structural and a dynamic point of view. In particular, ^{13}C spectra recorded by means of different pulse sequences, together with spectral fitting procedures and semiempirical chemical shift estimates, allowed us to make an assignment of the ^{13}C resonances to carbons belonging to different structural and diastereoisomeric environments. Moreover, the measurement of ^1H spin–lattice relaxation times in both the laboratory (T_1) and the rotating ($T_{1\rho}$) frame, as well as ^{13}C T_1 's, gave insight on the type of motions affecting

relaxation at temperatures ranging from 225 to 410 K, also allowing quantitative parameters to be extracted by applying suitable theoretical models.

Experimental Section

The hydrogenated oligo(cyclopentadiene) (HOCP) was a commercial sample produced by Esso Chemical ($M_w = 630$), showing a T_g of 70 °C, determined by DSC. The complete hydrogenation of the sample was assessed by means of ^{13}C NMR and IR spectra, which did not detect the presence of residual double bonds.

The NMR experiments were carried out on a Bruker AMX-300 WB spectrometer, working at 75.47 MHz for ^{13}C , equipped with a 4 mm CP-MAS probe. The 90° pulse was 3.5 μs .

In the single pulse excitation (SPE) experiments, a relaxation delay of 180 s was used in order to obtain quantitative spectra. The cross polarization (CP) experiments were performed using a contact time of 5 ms and a relaxation delay of 6 s. The spectral editing technique devised by Wu et al.³ was used with a contact time of 1 ms and a relaxation delay of 6 s.

Proton T_1 's were measured at different temperatures by detection in the time domain using an inversion–recovery technique followed by solid echo; at room temperature they were also measured by indirect ^{13}C detection using an inversion–recovery pulse sequence followed by ^1H – ^{13}C CP.⁴

Proton $T_{1\rho}$'s were measured via CP using the variable spin-lock time technique.⁵ Carbon T_1 's were measured by means of the Torchia technique.⁶

In all the experiments, apart from the directly detected proton T_1 measurement which was performed in static conditions, the magic angle spinning (MAS) rate was 7 kHz.

Because of heavy peak superpositions, the ^{13}C spectra were fitted using the SPORT-NMR software,⁷ which was also used to extract ^1H $T_{1\rho}$, ^1H T_1 , and ^{13}C T_1 relaxation times individually for all the peaks.

Results and Discussion

^{13}C Spectra. ^{13}C CP-MAS and SPE-MAS spectra recorded at room temperature are shown in Figure 1. No striking

[†] CNR. Fax: +39-050-502270. E-mail: claudia@indigo.icqem.pi.cnr.it.

[‡] Università degli Studi di Pisa. Fax: +39-050-918260. E-mail: marco@indigo.icqem.pi.cnr.it (M. Geppi), veracio@indigo.icqem.pi.cnr.it (C. A. Veracini), giuseppe@indigo.icqem.pi.cnr.it (G. Visalli).

[§] Heriot Watt University. E-mail: a.triolo@hw.ac.uk.

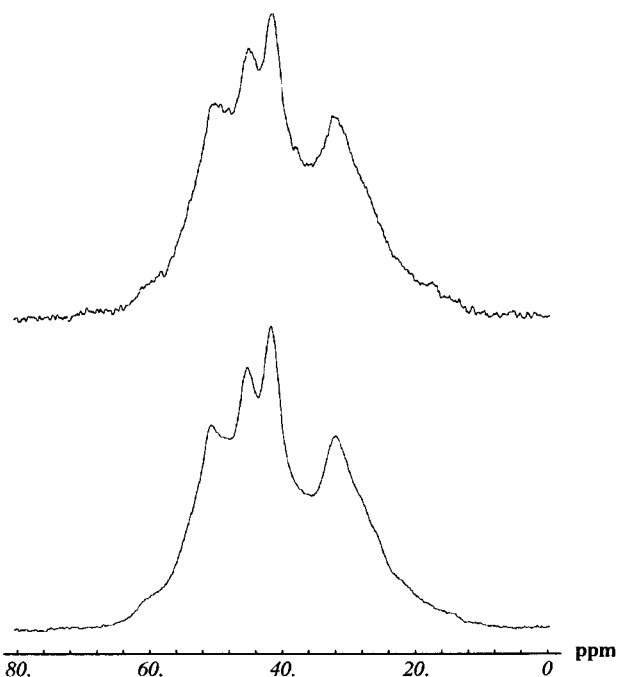


Figure 1. ^{13}C SPE-MAS (top) and CP-MAS (bottom) spectra of HOCP, recorded with 1200 and 4000 scans, respectively.

TABLE 1: Peak Labeling, Chemical Shifts and Integrals of the Fitted ^{13}C SPE-MAS Spectrum of HOCP at Room Temperature

peak	chemical shift (ppm)	peak integral (%)	peak	chemical shift (ppm)	peak integral (%)
A	59.5	4	E	37.4	7
B	49.7	30	F	32.0	18
C	44.9	8	G	25.8	17
D	41.2	16			

differences can be observed in the two spectra, indicating a similar cross-polarization dynamics for all the ^{13}C nuclei in the sample. The remarkably higher signal-to-noise ratio in the CP spectrum, even considering the different number of scans, indicates the presence, at room temperature, of strong ^{13}C – ^1H dipolar couplings, and therefore of a rigid phase, in agreement with a T_g of 70 °C for HOCP. The ^{13}C spectrum appears quite complex with a heavy superposition of several peaks. In order to try to assign all the resonances of the spectrum, we performed a spectral fitting of the quantitative SPE-MAS spectrum (see Figure 2 and Table 1): a good fitting was obtained using seven peaks. All the peaks were found to have a Gaussian line shape, with the exception of peak G (25.8 ppm), for which a Lorentzian line shape had to be used, thus suggesting a peculiar dynamic behavior for the carbon nuclei corresponding to this peak. However, the assignment of all the resonances to the different ^{13}C nuclei in the sample was not straightforward. In fact, despite the simplicity of the monomeric unit, which can be thought as a cyclopentane molecule, it must be pointed out that many nonequivalent carbon nuclei are present in HOCP, because of the presence of intermonomeric bonds in either 1,3 (structure I) or 1,2 (structure II) positions, which, in turn, can both result in either cis or trans arrangements; a further complication is ascribable to the presence of a remarkable amount of terminal groups (structure III, about 20%, since each oligomeric chain is composed of 10 monomeric units on average) (see Figure 3).

In order to try to unravel this situation, on one side we made use of a spectral editing technique capable of distinguishing between methylene and methine groups on the basis of their

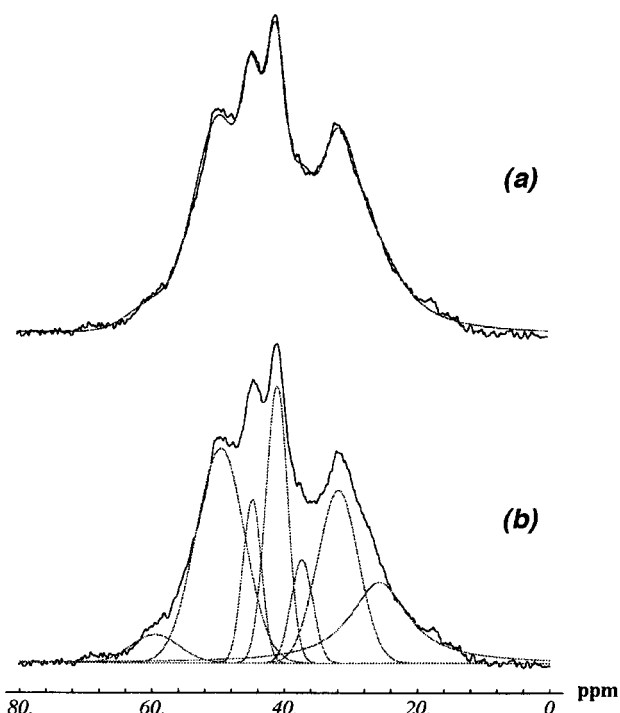


Figure 2. Fitting of the ^{13}C SPE-MAS spectrum: (a) experimental and fitted spectra; (b) experimental spectrum and single peaks of the fitted spectrum.

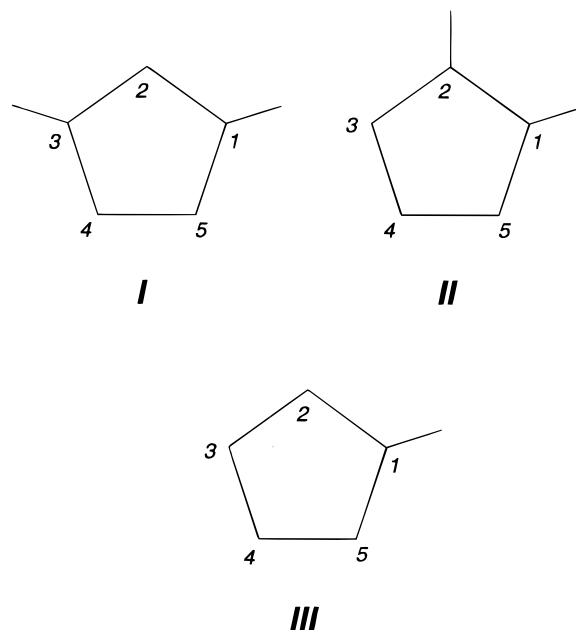


Figure 3. Structures of the different cyclopentane units present in HOCP.

different ^1H – ^{13}C cross-polarization time,³ and on the other side semiempirical chemical shifts were calculated starting from the values reported in the literature for 1,2- and 1,3-dimethylcyclopentane.⁸

The spectral editing experiment reported by Wu et al.³ gives rise to a spectrum where methylene peaks are inverted with respect to the normal CP spectrum, while methine peaks vanish. In an ideal case a suitable choice of the cross-depolarization time should give, for the methylene carbons, inverted signals having an integral equal to one-third of the corresponding integral of the CP spectrum; however, the degree of inversion at a fixed cross-depolarization time is strongly affected by the

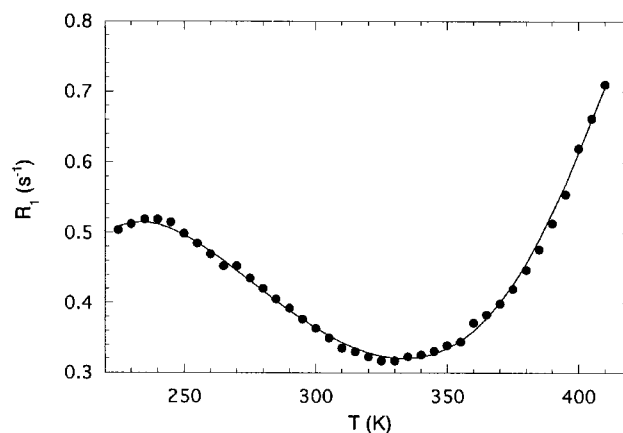
TABLE 2: Assignment of the Resonances of the ^{13}C SPE-MAS Spectrum to the Different Carbons of the Three Structures Shown in Figure 3^a

peak	exptl cs (ppm)	calcd cs (ppm)	carbon type
A	59.5	56.1–58.9	II-1,2t
B	49.7	49.9–53.2 (I-1,3) 51.0–53.8 (II-1,2) 49.7–49.8 (III-1)	I-1,3c,t; II-1,2c; III-1
C	44.9	42.5–47.2	I-2c,t
D	41.2	36.7–39.0 (I-4,5) 35.6–38.8 (II-3,5)	I-4,5c,t or II-3,5c,t
E	37.4	34.4–35.8	III-2,5
F	32.0	36.7–39.0 (I-4,5) 35.6–38.8 (II-3,5)	II-3,5c,t or I-4,5c,t
G	25.8	28.6–28.7 (II-4) 28.0 (III-3,4)	II-4c,t; III-3,4

^a In the “calcd cs” column the results of semiempirical calculations are reported, which have been performed starting from experimental chemical shifts of dimethylcyclopentanes and considering the changes induced by the substitution of methyl groups with cyclopentanes. Contributions up to δ position are considered. The chemical shift ranges reported refer to all the possible structural situations, combinations of I, II, and III adjacent monomeric units having been considered

^{13}C – ^1H dipolar coupling strength and should be expected, in principle, to be different for methylene carbons experiencing different structural and dynamic situations. The spectral editing spectrum of HOCP, recorded with a cross-depolarization time of 40 μs , revealed an increasing methylene character for peaks going toward low frequencies, with vanishing peaks A and B and the remaining peaks inverted, even though with different degrees of inversion, growing from C to G. The spectral editing technique thus allowed us to unambiguously assign peaks A and B to methine carbons and peak G to methylene carbons, whereas for the remaining peaks a methylene character is certain, but a partial methine contribution cannot be ruled out at this stage.

^{13}C chemical shifts of the different possible monomeric units in HOCP could be roughly predicted starting from the experimental chemical shifts of dimethylcyclopentane and taking into account the contributions due to the substitution of methyl groups with cyclopentanes. This approach must not be considered completely quantitative, not only because semiempirical calculations are not fully reliable, but also because these calculations refer to the liquid state, where individual conformations, in principle giving rise to different chemical shift values, are rapidly exchanged by fast motions, while this is no longer true in the solid state, where it could represent a non negligible source of error. However, from the comparison of experimental and calculated chemical shifts, and on the basis of their relative intensities, a more detailed spectral assignment could be attempted (see Table 2): the assignment of peaks A, B, C, and G seems sufficiently unambiguous, whereas the assignment of peaks D, E, and F to individual carbons is more difficult, since the calculated chemical shifts do not allow a reliable distinction among I-4,5, II-3,5, and III-2,5 carbons to be performed and therefore only a global assignment of these peaks is possible, even though peak E can be probably ascribed to III-2,5 on the basis of the integral value. In any case, peaks C–F should indeed arise from methylene carbons. The ratio between units I and II can be obtained from the integral values of peaks C and G: the integral of C (8%) is relative to one carbon of structure I only, while in G the subtraction of the contribution arising from III-3,4 (estimated in 8% of the global integral, given the average length of the oligomeric chain) gives a value of 9% for II-4; this indicates that the occurrence of structures I and II in HOCP

**Figure 4.** ^1H R_1 vs temperature trend and fitting curve obtained as described in the text, with the numerical parameters reported in Table 3.

is approximately equal. Moreover, by comparing the integrals of peaks A and B, and subtracting from the latter the contributions of structures I and III, a cis/trans ratio in structure II of about 2.5 can be inferred.

Relaxation Times. Measurements of proton and carbon spin–lattice relaxation times at different temperatures were performed in order to obtain insight on the dynamics of HOCP below and above its glass-transition temperature.

First of all, we investigated the trend of ^1H T_1 in the temperature range 225–410 K (the widest range experimentally accessible) with the aim of finding the number of dynamic processes responsible for relaxation. Proton spin–lattice relaxation times in the laboratory frame were measured by direct ^1H observation in the time domain, therefore obtaining a global answer from all the protons of the sample. A single-exponential decay as a function of the inversion–recovery variable delay was observed at all the temperatures. The trend of the spin–lattice relaxation rate (R_1) with the temperature is reported in Figure 4; it highlights the presence of at least two dynamic processes in the temperature range investigated. In fact, two typical R_1 curves can be recognized with maxima at about 237 K and above 410 K, with a minimum in proximity of the glass-transition temperature.

The ^1H T_1 measurement via CP, performed at room temperature, and followed by the application of spectral fitting procedures capable of extracting individual relaxation times for the different peaks present in the ^{13}C spectrum,⁷ allowed us to confirm the presence of a single T_1 value for all the protons of the sample, indicating that a complete averaging of intrinsic T_1 's takes place because of spin diffusion.

The impossibility of extracting more detailed information about the nature of these motional processes from proton spin–lattice relaxation times in the laboratory frame led us to resort to ^1H $T_{1\rho}$ and ^{13}C T_1 measurements at different temperatures. Proton relaxation times were determined through CP in order to exploit ^{13}C spectral resolution. In both cases, the spectral fitting procedures mentioned above were used, thus obtaining individual relaxation times for the different peaks. In the case of ^1H $T_{1\rho}$ the decay curves could always be well reproduced with a single-exponential function; all the peaks of the ^{13}C spectrum exhibited the same ^1H $T_{1\rho}$ within the experimental error (Figure 5), as a result of the complete averaging action exerted by spin diffusion also in a tens of angstroms scale. A remarkable decrease of relaxation time with increasing temperature, typical of the slow-motion side of a relaxation curve, can be observed. Since $T_{1\rho}$ minima occur at lower temperatures with

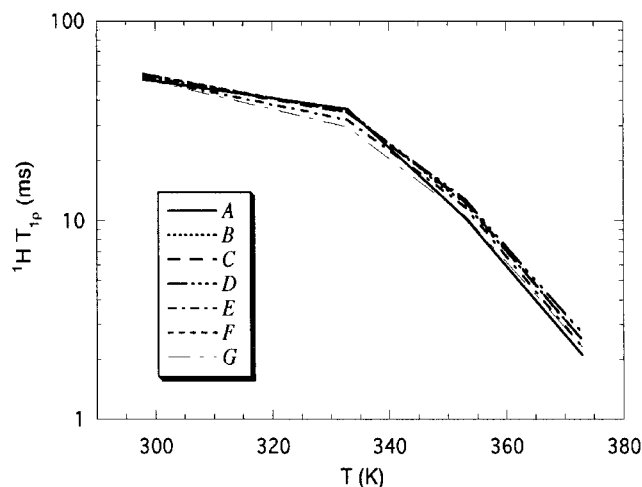


Figure 5. $^1\text{H } T_{1p}$ vs temperature trend for the different peaks of the ^{13}C spectrum.

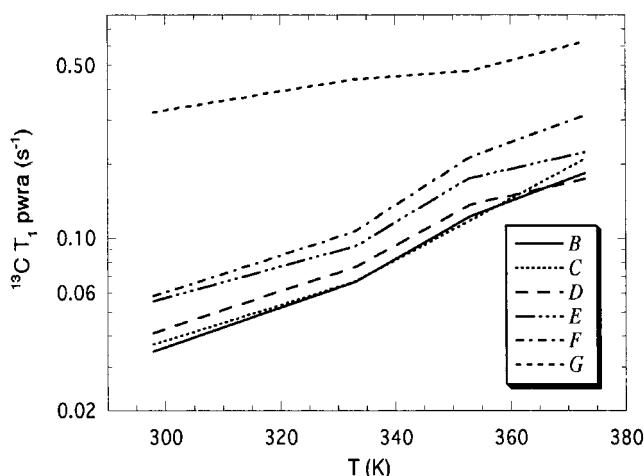


Figure 6. $^{13}\text{C } T_1$ pwra vs temperature trend for the different peaks of the ^{13}C spectrum.

respect to T_1 minima when ascribable to the same motional process, we can reasonably state that in the present case the spin–lattice relaxation in the rotating frame is mainly determined by the high-temperature motion previously observed in the $^1\text{H } T_1$ curve, but not much can be said about its nature.

Contrarily to what happens for proton relaxation times, the ^{13}C ones are not so strongly affected by spin diffusion, and therefore the relaxation behavior of the different nuclei more effectively reflects their dynamic environment. In this case, the relaxation behavior was not monoexponential, the experimental decay being better described by a sum of two exponential curves for all peaks. Therefore, comparison of the dynamic behavior of the different carbons was made on the basis of the “population-weighted rate average” (pwra) quantity, defined as

$$\text{pwra} = \sum_i \frac{w_i}{T_i}$$

where the sum runs over all the relaxation components and w_i is the fractional weight of the i th relaxation component. The pwra so obtained for the different peaks is reported in Figure 6. A peculiar behavior of peak G, which shows a remarkably larger pwra value, can be clearly observed over the whole temperature range investigated; it must be pointed out that while the ratio pwra(G)/pwra(B–F) is approximately 5–10 at room temperature, it decreases to 2–3 at 373 K. The different trend

observed for peak G is in agreement with the fact that only for this peak a Lorentzian line shape had to be used in the spectral fitting. The peculiar behavior of this peak, which arises from the superposition of signals of carbons belonging to terminal units and of carbon II-4, can be confidently ascribed to the latter, since peak E, assigned to carbons belonging to terminal monomeric units only, shows a behavior similar to all the other peaks. Consequently, in terms of relaxation in the megahertz region the most important dynamic process is a local, segmental motion mainly involving the carbon atom in position 4 of structure II. Previous studies performed on five-membered rings highlighted the presence in the solid state of ring pseudorotation (consisting in the interconversion between half-chair and bent conformations),⁹ occurring, for instance, in cyclopentane¹⁰ and *trans*-1,2-cyclopentanediol¹¹ even at very low temperatures. Taking into account that in HOCP the internal dynamics of the single monomeric units is remarkably hindered and constrained by the two intermonomeric bonds, which do not allow the whole ring to participate to an interconformer exchange, the closest motion could be the half-chair–half-chair inversion in structures II, involving the motion of carbon 4 below and above the plane formed by the remaining four carbons of the ring.

Since the dynamic range investigated by spin–lattice relaxation times is centered around the Larmor frequency, we can try to use the information arising from carbon T_1 's to assign the two motional processes observed in the $^1\text{H } T_1$ curve. The reduction with increasing the temperature of the peculiar carbon relaxation of peak G strongly suggests that the half-chair–half-chair inversion involving carbons II-4 represents the low-temperature motion observed in the $^1\text{H } T_1$ curve, while segmental main chain motions can be thought as the high-temperature dynamic process, in analogy with the motions usually taking place in polymers in correspondence of the glass transition, and in agreement with the reduction in ^{13}C spin–lattice relaxation differences at higher temperatures.

We tried to quantitatively describe the $^1\text{H } T_1$ trend reported in Figure 4 making use of available theoretical models. It is well-known that the proton spin–lattice relaxation time in the laboratory frame can be written as a function of spectral densities in the following way:

$$\frac{1}{T_1} = C[J_1(\omega_0) + 4J_2(2\omega_0)]$$

where C is a constant.

The spectral densities J_n can be expressed in terms of correlation times of the motion in different ways depending on the theoretical model considered, and, in turn, correlation times can be written as a function of temperature making use of other models.¹² We tried to reproduce the experimental curve using different models, and in particular Bloembergen–Purcell–Pound (BPP),¹³ Davidson–Cole (DC),¹⁴ and Cole–Cole (CC)¹⁵ for the J 's and an Arrhenius type behavior and Williams–Landel–Ferry (WLF)¹⁶ for the τ 's. In our case, the trend of the experimental relaxation times could be satisfactorily reproduced (see Figure 4) using BPP and CC for the low- and high-temperature motional processes, respectively, and an Arrhenius type behavior for the correlation times, according to the following equations:

$$J_{\text{BPP}}(\omega, \tau) = \frac{2\tau}{1 + \omega^2\tau^2}$$

$$J_{\text{CC}}(\omega, \tau, \delta) = \frac{2}{\omega} \sin\left(\frac{\delta\pi}{2}\right) \left[\frac{(\omega\tau)^\delta}{1 + (\omega\tau)^{2\delta} + 2(\omega\tau)^\delta \cos\left(\frac{\delta\pi}{2}\right)} \right]$$

TABLE 3: Dynamic Parameters Obtained from the Fitting of the ^1H T_1 Trend vs Temperature As Described in the Text

	τ_∞ (s)	E_a (kJ/mol)	δ
low-T motion	$(1.0 \pm 0.3) \times 10^{-13}$	37.4 ± 0.9	0.7
high-T motion	$(1.4 \pm 0.3) \times 10^{-12}$	14.1 ± 0.4	

The parameter δ in the CC model is a measure of the degree of correlated motion and of the distribution of correlation times.

The best-fitting parameters are reported in Table 3. The values obtained for activation energies are within the range usually found for dynamic processes of the type here considered, even though the models used, and in particular BPP and Arrhenius for the low- and high-temperature motions, are probably not the most suitable ones. However, while in the case of low-temperature motion the good fitting using BPP is probably due to the lack of sensitivity of the experimental data, for the high-temperature motion WLF gave physically unreasonable results. This indicates that WLF, which is known to be the most suitable model for motions associated with the glass transition of polymers, does not fully apply in the case of our oligomeric system. Moreover, the good fitting obtained using CC in the high-temperature region confirms that even for this oligomeric system the segmental main chain motions show a relevant degree of correlation, as usually found for polymers.

Conclusions

The analysis of the ^{13}C SPE-MAS spectrum of the oligomer HOCP using a spectral fitting routine allowed seven peaks to be distinguished; the assignment of these peaks was possible on the basis of semiempirical calculations. Approximately half of the nonterminal monomeric units in HOCP are found to have intermonomeric bonds in positions 1 and 2, with a cis/trans ratio of about 2.5, while the remaining monomers have intermonomeric bonds in positions 1 and 3.

^1H T_1 and $T_{1\rho}$'s and ^{13}C T_1 's at different temperatures allowed two motional processes to be revealed and characterized: at

lower temperatures relaxation is dominated by a local motion involving mainly carbon II-4, while at temperatures above T_g the dynamic process responsible for relaxation is a segmental main chain motion, characterized by a remarkable degree of correlated motion and distribution of correlation times.

References and Notes

- (1) Martuscelli, E.; Canetti, M.; Bonfatti, A. M.; Seves, A. *Polymer* **1991**, *32*, 641. Cimmino, S.; Di Pace, E.; Karasz, F. E.; Martuscelli, E.; Silvestre, C. *Polymer* **1993**, *34*, 972. Cimmino, S.; Martuscelli, E.; Silvestre, C. *Macromol. Symp.* **1994**, *78*, 115. Mendes, L. C.; Tavares, M. I. B.; Mano, E. B. *Polymer Testing* **1996**, *15*, 53. Caponetti, E.; Chillura Martino, D.; Cimmino, S.; Floriano, M. A.; Martuscelli, E.; Silvestre, C.; Triolo, R. *J. Mol. Struct.* **1996**, *383*, 75. Triolo, A.; Silvestre, C.; Cimmino, S.; Martuscelli, E.; Caponetti, E.; Triolo, R. *Polymer* **1998**, *39*, 1697. Triolo, A.; Lin, J. S.; Wignall, G. D.; Triolo, R. *Polymer*, in press. Crupi, V.; Majolino, D.; Migliardo, P.; Venuti, V.; Triolo, A.; Triolo, R. *Il Nuovo Cimento* **1998**, *20D*, 2437.
- (2) Triolo, A.; Lin, J. S.; Triolo, R. *Physica* **1998**, *A249*, 362.
- (3) Wu, X.; Burns, S. T.; Zilm, K. W. *J. Magn. Reson. A* **1994**, *111*, 29.
- (4) Weiss, G. H.; Gupta, R. K.; Ferretti, J. A.; Becker, E. D. *J. Magn. Reson.* **1980**, *37*, 369.
- (5) Sefcik, M. D.; Schaefer, J.; Stejskal, E. O.; McKay, R. A. *Macromolecules* **1980**, *13*, 1132.
- (6) Torchia, D. A. *J. Magn. Reson.* **1978**, *30*, 613.
- (7) Geppi, M.; Forte, C. *J. Magn. Reson.* **1999**, *137*, 177.
- (8) Christl, M.; Reich, H. J.; Roberts, J. D. *J. Am. Chem. Soc.* **1971**, *93*, 3463.
- (9) Kilpatrick, J. E.; Pitzer, K. S.; Spitzer, R. *J. Am. Chem. Soc.* **1947**, *69*, 2483.
- (10) Mack, J. W.; Torchia, D. A. *J. Phys. Chem.* **1991**, *95*, 4207 and references therein.
- (11) Riddell, F. G.; Cameron, K. S.; Holmes, S. A.; Strange, J. H. *J. Am. Chem. Soc.* **1997**, *119*, 7555.
- (12) Beckmann, P. A. *Phys. Rep.* **1988**, *171*, 85.
- (13) Bloembergen, N.; Purcell, E. M.; Pound, R. V. *Phys. Rev.* **1948**, *73*, 679.
- (14) Davidson, D. W.; Cole, R. H. *J. Chem. Phys.* **1951**, *19*, 1484.
- (15) Cole, K. S.; Cole, R. H. *J. Chem. Phys.* **1941**, *9*, 341.
- (16) Williams, M. L.; Landel, R. F.; Ferry, J. D. *J. Am. Chem. Soc.* **1955**, *77*, 3701.